



Cite this: DOI: 10.1039/d4cp02043j

 Received 16th May 2024,  
Accepted 3rd July 2024

DOI: 10.1039/d4cp02043j

rsc.li/pccp

# Effect of hydrostatic pressure on the supramolecular assembly of surfactant-cyclodextrin inclusion complexes†

 Larissa dos Santos Silva Araújo  ‡ and Leonardo Chiappisi  \*

The supramolecular assembly of simple colloids into complex, hierarchical structures arises from a delicate interplay of short-range directional and isotropic long-range forces. These assemblies are highly sensitive to environmental changes, such as temperature variations and the presence of specific molecules, making them promising candidates for nanomachine design. In this study, we investigate the effect of hydrostatic pressure, up to 1800 bar, on the supramolecular assemblies of cyclodextrin/surfactant complexes. Using small-angle neutron scattering, we demonstrate that while the overall structure of the supramolecular aggregates remains largely stable under pressure, the stiffness of the planar lattice formed by the inclusion complexes, the basic structural unit of the supramolecular assemblies, shows a fourfold increase between 250 and 1000 bar. These findings suggest that high-pressure studies can be exploited to better understand the mechanisms of supramolecular assembly processes, thereby aiding in the design of more robust and functional systems.

The assembly of small molecular entities into large, ordered complexes represents a fascinating yet highly challenging field of research. From the precise arrangement of proteins in viral capsids to the controlled polymerization of specific monomeric units forming supramolecular polymers, and the intricate functionality of molecular machines, supramolecular assemblies display a delicate interplay of forces and structures.<sup>1–3</sup> This domain is characterized by the dominance of strong, short-range directional interactions, such as hydrogen bonding,  $\pi$ - $\pi$  stacking, and lock-and-key binding. It is the strength, specificity, and directionality of these interactions which distinguish supramolecular assemblies from colloidal complexes governed by softer, more diffuse forces like dispersion and hydrophobic interactions. In contrast to the precise and localized interactions within supramolecular assemblies, colloidal

complexes are shaped by less specific, long-range forces. Understanding and controlling such processes hold great relevance for the design of new nanomaterials with advanced functionalities.<sup>4,5</sup>

Due to the ready availability of the components and the broad range of tuning parameters, the inclusion complexes formed between cyclodextrins and surfactants have been identified as excellent systems to investigate the fundamental principles governing the supramolecular assembly of simple molecules into large and complex structures.<sup>6–10</sup> The formation of these inclusion complexes is driven by the short-range, directional forces, such as hydrogen bonding, between the cyclodextrins and surfactants. In particular, hydrogen bonding between neighboring complexes leads to their crystallization into planar aggregates. Concurrently, the long-range electrostatic repulsion from the charged surfactant headgroup plays a significant role in influencing the overall assembly behavior. This interplay between short-range and long-range forces results in a rich variety of supramolecular structures, including capsids, vesicles, and multi-layered cylinders.

In this communication, we applied high hydrostatic pressure to probe volumetric effects on the supramolecular assembly of cyclodextrin-surfactant complexes. More broadly, hydrostatic pressure is a fundamental thermodynamic parameter that profoundly influences the physicochemical properties of colloidal systems, making it a powerful tool for investigating their structural or self-organization properties.<sup>11–14</sup> While some studies investigated the effect of high hydrostatic pressure on the inclusion complex formation between cyclodextrins and guest molecules,<sup>15,16</sup> the effect of pressure on the supramolecular assembly of the inclusion complexes remains unexplored.

In particular, herein we investigated the supramolecular assembly of inclusion complexes formed by  $\alpha$ -cyclodextrin (TCI Europe) and sodium pentaerythylene dodecyl carboxylate<sup>17</sup> (chemical formula given in the inset of Fig. 1, Kao Chemicals), with a cyclodextrin to surfactant molar mixing ratio of 2:1 and surfactant concentration of 3.5%<sub>vol</sub>. At the given experimental condition, all surfactant molecules are virtually threaded by cyclodextrin and the supramolecular assembly of the inclusion complexes at the

Institut Max von Laue - Paul Langevin (ILL), 71, avenue des Martyrs,  
38042 Grenoble, France. E-mail: chiappisi@ill.eu; Tel: +33476207953

† Electronic supplementary information (ESI) available: Additional experimental details; models used for the analysis of the scattering data; additional densitometric results. See DOI: <https://doi.org/10.1039/d4nj02243b>

‡ Present address: Univ. Grenoble Alpes, CNRS, LiPhy, Grenoble 38000, France.



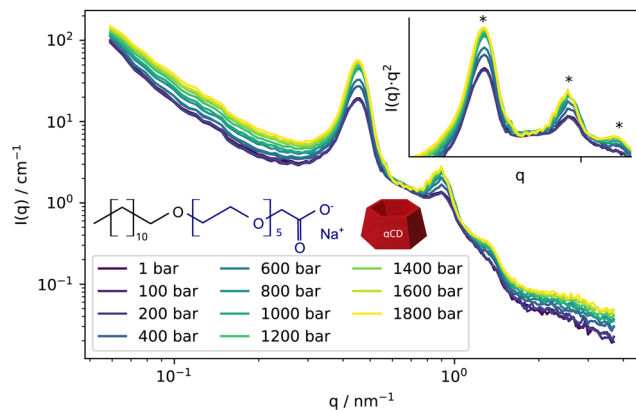


Fig. 1 Small-angle neutron scattering data from a  $\alpha$ CD- $C_{12}E_5CH_2$  COOH complexes as a function of the applied hydrostatic pressure. Inset shows region at mid- $q$  with the correlation peaks stemming from the multi-layered order within the aggregates in a  $I(q) \cdot q^2$  vs.  $q$  representation for improved readability. Peak positions of  $q^* = [0.45, 0.90, 1.35]$   $nm^{-1}$  are marked with\*.

structural scale 1–100 nanometers was probed by means of small-angle neutron scattering (SANS) experiments, performed on D33 at the Institut Laue-Langevin,<sup>18</sup> using a specifically designed high-pressure cell made in hardened copper-beryllium, and featuring fully transparent sapphire windows. The raw SANS data were correct for background contribution, the intensity normalized with respect to the incident beam, and the intensities isotropically averaged using the GRASP software package.<sup>19</sup> Samples were prepared in  $D_2O$  (Sigma-Aldrich) to allow for optimal contrast conditions, heated to 70 °C prior to fully solubilizing all components, and then slowly cooled down to 25 °C, the temperature at which this study was performed. Full details on the experiment are given in the (ESI†).

The SANS curves from supramolecular assemblies formed by the surfactant and cyclodextrins are depicted in Fig. 1. The data exhibit a distinctive pattern characteristic of these complexes assembling into multilayered structures, as indicated by the  $q^{-2}$  power law at low- $q$ , which is characteristic of the locally flat structure of the layers, and by the presence of multiple correlation peaks with Bragg peak position ratios of 1 : 2 : 3, typical of lamellar phases. Additionally, the gentle decay at high- $q$  suggests the finite thickness of the surfactant-cyclodextrin layer. As pressure increases up to 1800 bar, the overall shape of the scattering curve remains unchanged. However, there is a noticeable increase in the intensity of the correlation peaks, along with the emergence of the third-order reflection. This pressure-induced effect on the correlation peaks is further illustrated in the inset of Fig. 1, where the data are presented in a  $I(q) \cdot q^2$  vs.  $q$  representation.

Qualitatively, our interpretation suggests that, under the given experimental conditions of temperature, concentration, and pressure, the surfactant-cyclodextrin inclusion complex forms well-defined multilayered aggregates, consistent with findings from previous studies performed at ambient pressure.<sup>6–8,20–22</sup> While the scattering data do not indicate any significant structural changes in the assemblies, the strengthening of the correlation

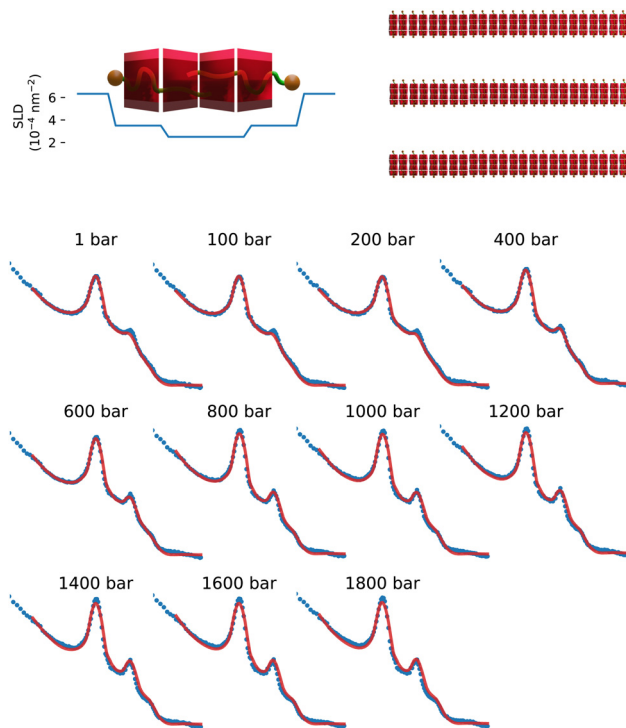


Fig. 2 Top: Scattering length density profile and schematic representation of the layer cross-section and schematic representation of the multilayered structure. Bottom, SANS scattering intensities from  $\alpha$ CD- $C_{12}E_5CH_2$  COONa complexes at different hydrostatic pressure values. Solid lines are best fits according to a model of stacked membranes, as described in the text. For absolute intensities and scattering vector values refer to Fig. 1.

peaks suggests an increase in order within the supramolecular assemblies as pressure rises.

To quantitatively assess the pressure-induced increase in order, we fitted the scattering data using a model of multilayer stacks. This model is defined using a form factor of core-shell, infinitely extended disks, coupled with a lamellar structure factor described within the modified Caillé theory.<sup>23,24</sup> Analytical expressions used are given in the ESI†. Fits were conducted in absolute units, utilizing molecular volumes and scattering length density values also detailed in the ESI†. The experimental data, along with the best fitting curves are shown in Fig. 2.

The cyclodextrin/surfactant layers are 3.3 nm thick, with the inner part composed of the surfactant chain and one cyclodextrin, while the outer part consists of the polar section of the surfactant, one cyclodextrin, and approximately 35%<sub>vol</sub> of water. The scattering length density profile aligns well with previous studies on similar cyclodextrin-surfactant assemblies.<sup>7,20</sup> Additional structural information can be extracted from the structure factor, including the interlayer spacing  $d_s$ , the average number of layers  $\langle N \rangle$ ; in a multilayered aggregate, and the Caillé parameter  $\eta_c$ , which is related to the rigidity of the stack. The Caillé parameter is given by:

$$\eta_c = \frac{\pi k_B T}{2d_s^2 \sqrt{BK}} \quad (1)$$



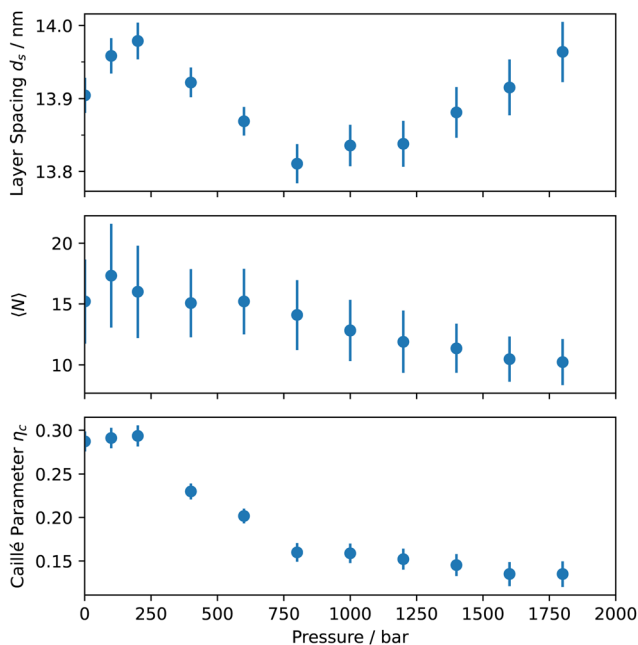


Fig. 3 Structural parameters obtained from the fit of the pressure dependent SANS data from  $\alpha$ CD- $C_{12}E_5$ CH<sub>2</sub>COO Na complexes. From top to bottom: the interlayer spacing, the average number of aggregate involved in one multilayered aggregate, and the Caillé parameter, related to the membrane stiffness. Error bars result from the uncertainty determined from the least squares minimization procedure.

where  $k_B T$  represents the thermal energy, and  $B$  and  $K$  denote the bulk compression modulus and the bending rigidity, respectively.

The pressure dependence of the most relevant parameters obtained from the analysis of the scattering data is illustrated in Fig. 3, which allows us to draw key conclusions regarding the effect of hydrostatic pressure on the supramolecular assemblies of cyclodextrin-surfactant complexes. As suggested by an initial qualitative analysis, the primary morphology of the multilayer aggregates appears unaffected by the applied hydrostatic pressure. This is evidenced by the constant interlayer spacing and, within its uncertainty, the constant number of layers. The constant interlayer spacing, which was shown to be strongly dependent on electrostatic repulsions between the layers,<sup>21</sup> indicates that pressure does not induce any significant change in the ionization condition or counterion condensation/release at the inclusion complex layer.

In contrast, a notable decrease in the Caillé parameter from approximately 0.3 at ambient pressure to below 0.13 at the highest pressure is observed. The Caillé parameter, reflecting membrane rigidity, significantly decreases between 250 and 750 bar, indicating molecular reorganization within this range. A decrease by a factor of 2 in the Caillé parameter corresponds to a fourfold increase in membrane rigidity. Although a single Caillé parameter value does not allow us to disentangle the bending and bulk compression modulus, we estimate that the bending modulus increases from about  $150 k_B T$  – a value reported by other authors at ambient pressure<sup>25</sup> – to up to  $600 k_B T$  at high pressure, assuming a constant bulk

compression modulus. Notably, other methods, such as small-angle X-ray scattering<sup>26</sup> or neutron spin-echo,<sup>27,28</sup> can provide more accurate absolute values for membrane rigidity.

In summary, these high-pressure SANS experiments have elucidated the structural behavior of supramolecular assemblies formed by  $\alpha$ -cyclodextrins and anionic surfactants within the 1–100 nm scale and up to pressure values of 1800 bar. Notably, while the overall dimensions and morphology of the aggregates remained unchanged, the application of hydrostatic pressure markedly enhanced the rigidity of the inclusion complex layer, resulting in a clear increase in order within the supramolecular architecture. In contrast, no significant pressure effects on the membrane rigidity were reported for phospholipid multilayered vesicles,<sup>29</sup> while a softening of polyoxyethylene-type nonionic surfactant bilayers in the  $L_\beta$  phase was found.<sup>30</sup>

Unfortunately, we can only speculate on the origin of the observed phenomenon. Based on previous densitometric experiments,<sup>21</sup> the application of hydrostatic pressure is not expected to shift the inclusion formation equilibrium at the investigated experimental conditions, with virtually all surfactant molecules threaded by the cyclodextrins. Furthermore, additional densitometric data provided in the ESI† do not highlight any significant volume effects associated with the supramolecular assembly of the inclusion complexes. Additionally, the application of hydrostatic pressure does not influence the electrostatic interactions between the inclusion complex layers, as indicated by the constant spacing between them. We hypothesize that the application of hydrostatic pressure might induce a change in the crystalline structure of the assemblies, triggering a transition towards a more compact and rigid structure. Future diffraction studies might confirm or disprove this hypothesis.

Finally, we present the first results on the effect of hydrostatic pressure on the structure of anionic surfactant and  $\alpha$ -cyclodextrin complexes. The observed enhancement in crystal rigidity and supramolecular ordering under pressure suggests potential structural reorganization within the crystalline lattice. While crystallography has traditionally been crucial in characterizing cyclodextrin inclusion complexes, particularly in pharmaceutical sciences where crystal form dictates drug activity and formulation, our results highlight the potential of high-pressure crystallography experiments to discover new or different crystal forms. These findings can be exploited for the formulation of more efficient drugs or to gain a deeper understanding of cyclodextrin chemistry.

Despite the inherent challenges associated with high-pressure experiments, we are optimistic that these preliminary findings underscore the significance of such studies. They hold promise for deepening our understanding of the supramolecular assembly of cyclodextrin inclusion complexes and their implications across diverse applications, including drug delivery and material science. For instance, the stability, solubility, or release profiles of supramolecular cyclodextrin-based drug delivery systems can be significantly affected by pressure-induced recrystallization processes.



## Author contributions

Larissa Dos Santos Silva Araujo: investigation, data curation, writing – review & editing. Leonardo Chiappisi: conceptualization, formal analysis, investigation, resources, writing – original draft, writing – review & editing, supervision, funding acquisition.

## Data availability

Data for this article, including the small-angle neutron scattering data are available at <https://doi.org/10.5291/ILL-DATA.9-12-703>.

## Conflicts of interest

There are no conflicts to declare.

## Acknowledgements

The authors acknowledge the ILL for allocated beamtime on the D33 SANS machine (DOI:10.5291/ILL-DATA.9-12-703) and the Partnership for Soft Condensed Matter (PSCM) for providing essential laboratory support, as well as the technical support provided by C. Payre, and J. Maurice. The high-pressure SANS cell was developed within the Integrated Infrastructure Initiative for Neutron Scattering and Muon Spectroscopy (NMI3-II) supported by the EU 7th Framework Programme (FP7).

## References

- 1 S. Erbas-Cakmak, D. A. Leigh, C. T. McTernan and A. L. Nussbaumer, *Chem. Rev.*, 2015, **115**, 10081–10206.
- 2 D. Law-Hine, A. K. Sahoo, V. Bailleux, M. Zeghal, S. Prevost, P. K. Maiti, S. Bressanelli, D. Constantin and G. Tresset, *J. Phys. Chem. Lett.*, 2015, **6**, 3471–3476.
- 3 L. Cera, L. Chiappisi, C. Böttcher, A. Schulz, S. Schoder, M. Gradzielski and C. A. Schalley, *Adv. Mater.*, 2017, **29**, 1604430.
- 4 Y. M. Zhang, Y. H. Liu and Y. Liu, *Adv. Mater.*, 2020, **32**, 1–19.
- 5 S. Dutta Choudhury and H. Pal, *Phys. Chem. Chem. Phys.*, 2020, **22**, 23433–23463.
- 6 C. Wu, Q. Xie, W. Xu, M. Tu and L. Jiang, *Curr. Opin. Colloid Interface Sci.*, 2019, **39**, 76–85.
- 7 S. Ouhajji, J. Landman, S. Prevost, L. Jiang, A. P. Philipse and A. V. Petukhov, *Soft Matter*, 2017, **13**, 2421–2425.
- 8 J. Landman, S. Ouhajji, S. Prevost, T. Narayanan, J. Groenewold, A. P. Philipse, W. K. Kegel and A. V. Petukhov, *Sci. Adv.*, 2018, **4**, eaat1817.
- 9 L. dos Santos Silva Araújo, G. Lazzara and L. Chiappisi, *Adv. Colloid Interface Sci.*, 2021, **289**, 102375.
- 10 L. Jiang, Y. Yan and J. Huang, *Adv. Colloid Interface Sci.*, 2011, **169**, 13–25.
- 11 C. M. Papadakis, B. J. Niebuur and A. Schulte, *Langmuir*, 2024, **40**, 1–20.
- 12 S. Micciulla, P. Gutfreund, M. Kandu and L. Chiappisi, *Macromolecules*, 2023, **56**, 1177–1188.
- 13 H. Mizuno and G. Fukuhara, *Acc. Chem. Res.*, 2022, **55**, 1748–1762.
- 14 L. Smeller, *Biochim. Biophys. Acta, Protein Struct. Mol. Enzymol.*, 2002, **1595**, 11–29.
- 15 X. Hu, B. Wei, H. Li, C. Wu, Y. Bai, X. Xu, Z. Jin and Y. Tian, *Carbohydr. Polym.*, 2012, **90**, 1193–1196.
- 16 A. Abou-Hamdan, P. Bugnon, C. Saudan, P. G. Lye and A. E. Merbach, *J. Am. Chem. Soc.*, 2000, **122**, 592–602.
- 17 L. Chiappisi, *Adv. Colloid Interface Sci.*, 2017, **250**, 79–94.
- 18 C. D. Dewhurst, I. Grillo, D. Honecker, M. Bonnaud, M. Jacques, C. Amrouni, A. Perillo-Marcone, G. Manzin and R. Cubitt, *J. Appl. Crystallogr.*, 2016, **49**, 1–14.
- 19 C. D. Dewhurst, *J. Appl. Crystallogr.*, 2023, **56**, 1595–1609.
- 20 S. Yang, Y. Yan, J. Huang, A. V. Petukhov, L. M. J. Kroon-Batenburg, M. Drechsler, C. Zhou, M. Tu, S. Granick and L. Jiang, *Nat. Commun.*, 2017, **8**, 15856.
- 21 L. dos Santos Silva Araújo, L. Watson, D. A. K. Traore, G. Lazzara and L. Chiappisi, *Soft Matter*, 2022, **8**, 6529–6537.
- 22 L. dos Santos Silva Araújo, G. Lazzara and L. Chiappisi, *Soft Matter*, 2023, **19**, 1523–1530.
- 23 R. Zhang, S. Tristram-Nagle, W. Sun, R. L. Headrick, T. C. Irving, R. M. Suter and J. F. Nagle, *Biophys. J.*, 1996, **70**, 349–357.
- 24 A. Caillé, *C. R. Seances Acad. Sci., Ser. B*, 1972, **274**, 891–893.
- 25 T. Komarova, T. Zinn, T. Narayanan, A. V. Petukhov and J. Landman, *arXiv*, 2023, Preprint, arXiv:2312.05637, DOI: [10.48550/arXiv.2312.05637](https://doi.org/10.48550/arXiv.2312.05637).
- 26 G. Pabst, A. Hodzic, J. Štrancar, S. Danner, M. Rappolt and P. Laggnier, *Biophys. J.*, 2007, **93**, 2688–2696.
- 27 L. Chiappisi, I. Hoffmann and M. Gradzielski, *J. Colloid Interface Sci.*, 2022, **627**, 160–167.
- 28 I. Hoffmann, *Colloid Polym. Sci.*, 2014, 2053–2069.
- 29 S. R. Al-Ayoubi, P. K. Schinkel, M. Berghaus, M. Herzog and R. Winter, *Soft Matter*, 2018, **14**, 8792–8802.
- 30 T. Takano, Y. Kawabata, T. Suzuki and T. Kato, *J. Phys. Chem. B*, 2015, **119**, 11656–11663.

